Published in final edited form as:
Nat Genet. ; 44(3): 334–337. doi:10.1038/ng.1067.

Common Variants near *MBNL1* and *NKX2-5* are Associated with Infantile Hypertrophic Pyloric Stenosis

Bjarke Feenstra[1,*], **Frank Geller**[1,*], **Camilla Krogh**[1], **Mads V. Hollegaard**[2], **Sanne Gørtz**[1], **Heather A. Boyd**[1], **Jeffrey C. Murray**[3], **David M. Hougaard**[2], and **Mads Melbye**[1]

[1]Department of Epidemiology Research, Statens Serum Institut, Copenhagen, Denmark

[2]Section of Neonatal Screening and Hormones, Statens Serum Institut, Copenhagen, Denmark

[3]Department of Pediatrics, University of Iowa, Iowa City, Iowa

Infantile Hypertrophic Pyloric Stenosis (IHPS) is a severe condition characterized by hypertrophy of the pyloric sphincter muscle. We conducted a genome-wide association study (GWAS) on 1,001 surgery-confirmed cases and 2,401 controls from Denmark. The 6 most strongly associated loci were tested in a replication set of 796 cases and 876 controls. Three SNPs reached genome-wide significance. Rs11712066 (odds ratio (OR) = 1.61, $P = 1.5 \times 10^{-17}$) on 3p25.1 is located 150 kb upstream of *MBNL1*, which regulates splicing transitions occurring shortly after birth. The second SNP, rs573872 (OR = 1.41, $P = 4.3 \times 10^{-12}$), maps to an intergenic region on 3p25.2 some 1.3 Mb downstream of *MBNL1*. The third SNP, rs29784 (OR = 1.42, $P = 1.5 \times 10^{-15}$) on 5q35.2, is 64 kb downstream of *NKX2-5*, which is involved in development of cardiac muscle tissue and embryonic gut development.

IHPS is a severe condition of infancy in which hypertrophy of the pyloric sphincter smooth muscle leads to obstruction of the gastric outlet. Symptoms typically appear between 2 and 8 weeks after birth [1] and include non-bilious projectile vomiting that progresses to dehydration, weight loss and hypochloremic, hypokalemic metabolic alkalosis. Treatment may require correction of electrolyte disturbances and curative surgical incision of the pyloric sphincter muscle. The incidence of IHPS among whites is 1.5 to 3 per 1000 live births [2, 3], and it is the most common condition requiring surgery in the first months of life [4]. There is a pronounced male excess in the incidence of IHPS, with affected boys outnumbering girls in a 4 to 1 ratio [5, 6].

While environmental risk factors such as exposure to erythromycin [7] and bottle feeding [8] have been reported, IHPS also aggregates strongly in families [6]. In a population-based cohort study of almost 2 million children, there was a nearly 200-fold increased risk in

Correspondence should be addressed to B.F. (fee@ssi.dk) or M.M. (mme@ssi.dk). .
*these authors contributed equally

AUTHOR CONTRIBUTIONS B.F., F.G. and M.M. wrote the first draft of the paper. B.F. and F.G analyzed the data. M.V.H. and D.M.H. performed the experiments. C.K., S.G., J.C.M. and H.A.B. contributed by collecting phenotype data, providing genotype data, and/or giving advice on interpretation of results. B.F., F.G. and M.M. planned and supervised the work. All authors contributed to writing the final manuscript.

COMPETING FINANCIAL INTERESTS Statens Serum Institut has filed a priority patent application at the Danish Patent and Trademark Office on the use of genetic profiling to identify newborns at risk of IHPS, which contains subject matter drawn from the work also published here.

URLs 1000 Genomes Project, http://www.1000genomes.org/; Chicago eQTL Browser, http://eqtl.uchicago.edu/cgi-bin/gbrowse/eqtl/; GWAS Catalog, http://www.genome.gov/gwastudies/; HapMap, http://www.hapmap.org/; LocusZoom, http://csg.sph.umich.edu/locuszoom/; MACH, http://www.sph.umich.edu/csg/abecasis/MACH/index.html; PLINK, http://pngu.mgh.harvard.edu/~purcell/plink/; UCSC Genome Browser, http://genome.ucsc.edu/cgi-bin/hgGateway/.

monozygotic twins, a 20-fold increased risk among siblings and the heritability was estimated to be 87% [3]. IHPS is generally regarded as a complex disease with multiple genetic and environmental factors contributing to disease pathogenesis [2, 9]. Several linkage and candidate gene studies have been conducted (review by Panteli[10]), but there are no genetic variants with replicated association findings.

To identify IHPS susceptibility loci, we analyzed the association between the disease and 523,420 SNPs in 1,001 cases and 2,401 controls of Danish descent. All IHPS cases were surgery-confirmed, singletons, and without major congenital malformations (see Supplementary Note and Supplementary Table 1 for details). We identified six loci associated at $P<=1\times10^{-6}$ (Figure 1 and Supplementary Figure 1). To confirm the observed associations we genotyped and tested the most significant SNP at each of the six loci in a replication sample of 796 cases (also surgery-confirmed) and 876 controls, all of Danish descent (see Supplementary Table 2 for basic characteristics of the discovery and replication sample). Three loci replicated with combined p-values $< 1 \times 10^{-11}$, two loci were close to nominal significance in the replication stage but remained suggestive, and one locus failed to replicate (Table 1). Genotyping of one additional SNP at each locus produced essentially the same results (Supplementary Table 3) and correction for possible population substructure did not influence our findings (Supplementary Table 4). We found no evidence of interaction between the top three loci (data not shown). Assuming a multifactorial liability-threshold model [11], the three confirmed SNPs collectively explain 1.8% of the variance in liability to IHPS. Considering the combined number of risk alleles across the three SNPs, the 8% of children carrying five or six risk alleles were at almost five times higher risk of IHPS compared to the 8% with zero or one alleles (OR = 4.91, 95% confidence interval 3.59 to 6.71).

The first genome-wide significant variant, rs11712066 (OR = 1.61, $P = 1.5 \times 10^{-17}$), is located 150 kb upstream of *MBNL1* on 3q25.1 with a recombination hotspot between the SNP and the gene (Figure 2a). The closest genes on the other side, *AADAC* and *SUCNR1* are about 250 kb centromeric. The second identified SNP, rs573872 (OR = 1.41, $P = 4.3 \times 10^{-12}$) on 3q25.2, lies in a gene desert some 1.3 Mb downstream of *MBNL1* and the closest genes are *C3orf79* about 250 kb centromeric and *ARHGEF26* about 370 kb telomeric (Figure 2b). Further centromeric between rs573872 and *MBNL1* there are two small genes *P2RY1* and *RAP2B*. The third genome-wide significant variant, rs29784 (OR = 1.42, $P = 1.5 \times 10^{-15}$), is located on chromosome 5q35.2 between *BNIP1* and *NKX2-5* in a linkage disequilibrium (LD) block that contains both genes (Figure 2c).

To explore the association signals further, we imputed unobserved genotypes in the three confirmed regions based on the Interim Phase I release of the 1000 Genomes Project[12] (see Online Methods and Supplementary Note for details of imputation). A large number of imputed SNPs showed strong association; at the 3q25.1 and 3q25.2 loci, the strongest associated imputed SNPs had P values at the same order of magnitude as the top genotyped SNP; at the 5q35.2 locus the best imputed SNP rs40264 (OR = 1.49, $P = 1.2 \times 10^{-12}$, r^2 to rs29784 = 0.85) had a P value two orders of magnitude smaller than that of rs29784 (Supplementary Table 5, Supplementary Figures 2–4). Most associated imputed SNPs were in tight LD with the top genotyped SNP of the region, and when accounting for the genotyped SNP, we observed no $P < 10^{-5}$ (Supplementary Figures 2–4). A long-range haplotype analysis across the 3p25.1 and 3p25.2 loci did not reveal rare haplotypes with high odds ratio (Supplementary Note and Supplementary Table 6).

In order to investigate the possible functional impact of the associations, we considered all 294 genotyped or imputed SNPs with $P < 10^{-6}$, and searched for functional predictions for these SNPs. 19 of these SNPs were located in genes (*C5orf41* and *BNIP1*), but all were

intronic (Supplementary Table 5). A search of the eQTL browser (see URLs) for the 294 SNPs did not reveal any association to gene expression. Next, we explored ENCODE data[13] (using the UCSC genome browser NCBI build 36; see URLs) from chromatin immunoprecipitation sequencing (ChIP-seq) experiments, which showed a 23 kb region of histone modification for H3K36me3 that directly overlies rs11712066. At the 5q35.2 locus there are wider regions of histone modification for H3K27me3 and H3K36me3, both covering rs29784. While histone modification can mark distant-acting enhancers[14], speculations on specific mechanisms are premature. A search of the GWAS catalog (see URLs) showed that rs251253 on 5q32.2 (OR = 1.34, $P = 6.0 \times 10^{-7}$, r^2 to rs29784 = 0.49) is associated with the electrocardiographic PR interval[15]. The functional basis for the association is, however, unknown.

In light of the pronounced excess risk of IHPS in males, we also carried out sex-specific analysis of the data (Supplementary Table 7). The three genome-wide significant SNPs showed no evidence of heterogeneity of effects between sexes. Although rs2228671 on chromosome 19p13.2 failed to replicate, the strong effect in boys (OR = 1.54, $P = 7.6 \times 10^{-8}$) and absence of effect in girls (OR = 0.91, $P = 0.53$) warrants further study.

The three confirmed SNPs map to regions where *MBNL1* and *NKX2-5* are the strongest functional candidates for IHPS. Members of the muscleblind protein family are important regulators of alternative splicing[16] and almost all human multiexon genes undergo alternative splicing [17]. In the early post-natal period, splicing transitions from fetal to adult protein isoforms are essential for the extensive remodeling of muscle tissue that occurs as a part of normal development[18]. In studies of mouse heart and skeletal muscle development, *Mbnl1* has been shown to control a set of temporally correlated splicing transitions that occur within the first 3 weeks of post-natal life [19, 20]. Additionally, expression levels of *Mbnl1* show distinct temporal changes in the early post-natal period correlated with the splicing transitions [18, 19]. The intriguing observation that IHPS occurs almost exclusively between 2 and 8 weeks after birth points to a possible role for misregulation of *MBNL1*-controlled splicing transitions in the etiology of IHPS. The importance of *MBNL1* for normal development of muscle tissue is highly evident in myotonic dystrophy, where loss of function of MBNL1 (caused by mutant *DMPK* mRNA), and consequent aberrant alternative splicing for many different pre-mRNAs, has a pivotal role in the pathogenesis of the disease [20].

NKX2-5 at chromosome 5q35.2 encodes the homeobox transcription factor NKX2-5, which is essential for normal heart formation and development [21]. In humans, a range of *NKX2-5* mutations have been identified that cause different congenital heart defects including atrial septal defects with or without atrioventricular block, isolated ventricular septal defects, and tetralogy of Fallot [22]. Although *NKX2-5* is not expressed in adult extracardiac tissues [23] studies of embryonic gut development have shown that *NKX2-5* is crucial for the formation of pyloric sphincter muscle tissue [24-26]. In both chicken and mouse, *Nkx2-5* expression occurs in a sharply defined ring of mesenchyme at the junction between the foregut and midgut on specific days of embryonic development [23, 24, 26]. Furthermore, repression of *Nkx2-5* activity in the pyloric sphincter region results in loss of the pyloric sphincter endodermal phenotype; conversely, formation of pyloric sphincter-like epithelium in other parts of the gizzard (the equivalent of the stomach in the chicken) can be induced by ectopic expression of *Nkx2-5* via a retroviral vector [25].

Further experimental studies are needed to uncover the contributions of, e.g., distant-acting enhancers, alternative splicing, or other potential mechanisms to the molecular etiology of IHPS. Although biopsies of pyloric sphincter muscle tissue would be difficult to obtain, comparison of *NKX2-5* expression levels in such tissue from IHPS patients with that from

age-matched controls would be interesting, as might be analysis of alternative splicing in pyloric sphincter muscle tissue using mRNA sequencing.

In conclusion, we identified three independent, robustly associated loci for IHPS. The findings point to two candidate genes, involved in regulation of alternative splicing, cardiac muscle development, and embryonic gut development. Further functional investigation of the associations identified here will illuminate the biological mechanisms behind this enigmatic condition and may lead to new approaches for screening, prevention or treatment.

METHODS

SUBJECTS

Eligible IHPS cases were defined as children who 1) in their first year of life had a pyloromyotomy 2) were singletons 3) did not have any major malformations, and 4) were of Danish ancestry. In addition, we excluded severe pregnancy complications (see Supplementary Note for details about selection criteria). In the discovery stage, samples from 1,001 cases were selected and successfully genotyped. The control group consisted of 2,401 non-affected Danish children. Apart from IHPS affection status, the selection criteria were the same as for the cases. For the replication stage, we used 796 cases and 876 controls drawn from the same population using the same case and control definitions as in the discovery stage. The sex distribution was similar in the discovery and replication samples, but replication cases were born an average of 6 years earlier than discovery cases (Supplementary Table 2). The study was approved by the Scientific Ethics Committee for the Capital City Region (Copenhagen) and the Danish Data Protection Agency.

GENOTYPING AND QUALITY CONTROL

All samples were drawn from the Danish Newborn Screening Biobank and the Danish National Birth Cohort biobank, both of which are part of the Danish National Biobank. Sampling and genotyping (using the Illumina Human 660W-Quadv1_A chip) was undertaken in two rounds (see Supplementary Note for details). In total, genotypes for 559,390 SNPs were released in both genotyping rounds. For the association analysis, we used 523,420 SNPs; the other SNPs were excluded based on a missing rate >5%, deviation from Hardy-Weinberg equilibrium in controls ($P<10^{-3}$), minor allele frequency <1%, or discrepancies ($P<10^{-7}$) in allele frequencies between the two genotyping rounds. Genotyping of replication samples was performed on two correlated SNPs at each of the 6 most significantly associated loci from the discovery stage at deCODE Genetics using the Centaurus platform (Nanogen). We regenotyped 147 discovery stage samples and observed 100% concordance in a total of 1604 genotypes.

STATISTICAL ANALYSIS

For the SNPs passing quality control, we used PLINK [28] to test for differences in allele frequencies between cases and controls for the discovery samples overall and stratifying by sex. P values were corrected by genomic control [29] using estimated genomic inflation factors of 1.06 in the combined discovery data, 1.04 in the analysis restricted to boys and 1.02 in the analysis for girls. We carried out combined analysis of the discovery and replication data using the inverse variance method as implemented in METAL [30] and tested for heterogeneity of the discovery and replication results using the I^2 statistic [31]. Using the combined discovery and replication data, we tested for interaction effects between the top six loci by including risk allele count at each locus in a logistic regression model together with pair-wise interaction terms. We also used the combined data to estimate the proportion of variance in the liability to IHPS explained by each of the top SNPs [32].

GENOTYPE IMPUTATION

We imputed unobserved genotypes in the three confirmed regions using phased haplotypes from the Interim Phase I release of the 1000 Genomes Project [12]. Imputation was done in a two step procedure. In a first pre-phasing step, we used MaCH [33] to estimate haplotypes for the IHPS study samples. In a second step, we imputed missing alleles for additional SNPs directly onto these phased haplotypes using Minimac [33]. All imputed SNPs with imputation quality r^2 >0.30 were tested for association with IHPS in a logistic regression of disease status on imputed allele dosage (to account for imputation uncertainty) using mach2dat [33]. In addition, we carried out analyses conditioning on the genotype of the confirmed genotyped SNP in each region. (See Supplementary Note for additional information.)

Supplementary Material

Refer to Web version on PubMed Central for supplementary material.

Acknowledgments

This study was supported in part by grants from the Lundbeck Foundation (R34-A3931), the Novo Nordisk Foundation and the Danish Medical Research Council (271-06-0628). The GWAS data for the control samples were generated for our study of preterm birth within the GENEVA consortium with funding provided through the NIH Genes, Environment and Health Initiative (GEI: U01HG004423). Assistance with genotype cleaning and general study coordination for the preterm birth project was provided by the GENEVA Coordinating Center (U01HG004446). Genotyping was performed at Johns Hopkins University Center for Inherited Disease Research, with support from the NIH GEI (U01HG004438).

REFERENCES

1. Ranells JD, Carver JD, Kirby RS. Infantile hypertrophic pyloric stenosis: epidemiology, genetics, and clinical update. Adv. Pediatr. 2011; 58:195–206. [PubMed: 21736982]
2. Mitchell LE, Risch N. The genetics of infantile hypertrophic pyloric stenosis. A reanalysis. Am J Dis. Child. 1993; 147:1203–1211.
3. Krogh C, et al. Familial aggregation and heritability of pyloric stenosis. JAMA. 2010; 303:2393–2399. [PubMed: 20551410]
4. Chung E. Infantile hypertrophic pyloric stenosis: genes and environment. Arch Dis. Child. 2008; 93:1003–1004. [PubMed: 19028966]
5. Schechter R, Torfs CP, Bateson TF. The epidemiology of infantile hypertrophic pyloric stenosis. Paediatr. Perinat. Epidemiol. 1997; 11:407–427. [PubMed: 9373863]
6. MacMahon B. The continuing enigma of pyloric stenosis of infancy: a review. Epidemiology. 2006; 17:195–201. [PubMed: 16477261]
7. Honein MA, et al. Infantile hypertrophic pyloric stenosis after pertussis prophylaxis with erythromcyin: a case review and cohort study. Lancet. 1999; 354:2101–2105. [PubMed: 10609814]
8. Pisacane A, et al. Breast feeding and hypertrophic pyloric stenosis: population based case-control study. BMJ. 1996; 312:745–746. [PubMed: 8605461]
9. Chakraborty R. The inheritance of pyloric stenosis explained by a multifactorial threshold model with sex dimorphism for liability. Genet. Epidemiol. 1986; 3:1–15. [PubMed: 3957000]
10. Panteli C. New insights into the pathogenesis of infantile pyloric stenosis. Pediatr. Surg. Int. 2009; 25:1043–1052. [PubMed: 19760199]
11. Falconer DS. The inheritance of liability to certain diseases, estimated from the incidence among relatives. Annals of Human Genetics. 1965; 29:51–76.
12. A map of human genome variation from population-scale sequencing. Nature. 2010; 467:1061–1073. [PubMed: 20981092]
13. Myers RM, et al. A user's guide to the encyclopedia of DNA elements (ENCODE). PLoS. Biol. 2011; 9:e1001046. [PubMed: 21526222]

14. Visel A, Rubin EM, Pennacchio LA. Genomic views of distant-acting enhancers. Nature. 2009; 461:199–205. [PubMed: 19741700]
15. Pfeufer A, et al. Genome-wide association study of PR interval. Nat. Genet. 2010; 42:153–159. [PubMed: 20062060]
16. Ho TH, et al. Muscleblind proteins regulate alternative splicing. EMBO J. 2004; 23:3103–3112. [PubMed: 15257297]
17. Pan Q, Shai O, Lee LJ, Frey BJ, Blencowe BJ. Deep surveying of alternative splicing complexity in the human transcriptome by high-throughput sequencing. Nat. Genet. 2008; 40:1413–1415. [PubMed: 18978789]
18. Bland CS, et al. Global regulation of alternative splicing during myogenic differentiation. Nucleic Acids Res. 2010; 38:7651–7664. [PubMed: 20634200]
19. Kalsotra A, et al. A postnatal switch of CELF and MBNL proteins reprograms alternative splicing in the developing heart. Proc. Natl. Acad. Sci. U. S. A. 2008; 105:20333–20338. [PubMed: 19075228]
20. Lin X, et al. Failure of MBNL1-dependent post-natal splicing transitions in myotonic dystrophy. Hum. Mol. Genet. 2006; 15:2087–2097. [PubMed: 16717059]
21. Fu Y, Yan W, Mohun TJ, Evans SM. Vertebrate tinman homologues XNkx2-3 and XNkx2-5 are required for heart formation in a functionally redundant manner. Development. 1998; 125:4439–4449. [PubMed: 9778503]
22. Reamon-Buettner SM, Borlak J. NKX2-5: an update on this hypermutable homeodomain protein and its role in human congenital heart disease (CHD). Hum. Mutat. 2010; 31:1185–1194. [PubMed: 20725931]
23. Kasahara H, Bartunkova S, Schinke M, Tanaka M, Izumo S. Cardiac and extracardiac expression of Csx/Nkx2.5 homeodomain protein. Circ. Res. 1998; 82:936–946. [PubMed: 9598591]
24. Smith DM, Tabin CJ. BMP signalling specifies the pyloric sphincter. Nature. 1999; 402:748–749. [PubMed: 10617196]
25. Smith DM, Nielsen C, Tabin CJ, Roberts DJ. Roles of BMP signaling and Nkx2.5 in patterning at the chick midgut-foregut boundary. Development. 2000; 127:3671–3681. [PubMed: 10934012]
26. Self M, Geng X, Oliver G. Six2 activity is required for the formation of the mammalian pyloric sphincter. Dev. Biol. 2009; 334:409–417. [PubMed: 19660448]
27. Pruim RJ, et al. LocusZoom: regional visualization of genome-wide association scan results. Bioinformatics. 2010; 26:2336–2337. [PubMed: 20634204]
28. Purcell S, et al. PLINK: a tool set for whole-genome association and population-based linkage analyses. Am. J. Hum. Genet. 2007; 81:559–575. [PubMed: 17701901]
29. Devlin B, Roeder K. Genomic control for association studies. Biometrics. 1999; 55:997–1004. [PubMed: 11315092]
30. Willer CJ, Li Y, Abecasis GR. METAL: fast and efficient meta-analysis of genomewide association scans. Bioinformatics. 2010; 26:2190–2191. [PubMed: 20616382]
31. Higgins JP, Thompson SG. Quantifying heterogeneity in a meta-analysis. Stat. Med. 2002; 21:1539–1558. [PubMed: 12111919]
32. So HC, Gui AH, Cherny SS, Sham PC. Evaluating the heritability explained by known susceptibility variants: a survey of ten complex diseases. Genet. Epidemiol. 2011; 35:310–317. [PubMed: 21374718]
33. Li Y, Willer CJ, Ding J, Scheet P, Abecasis GR. MaCH: using sequence and genotype data to estimate haplotypes and unobserved genotypes. Genet. Epidemiol. 2010; 34:816–834. [PubMed: 21058334]

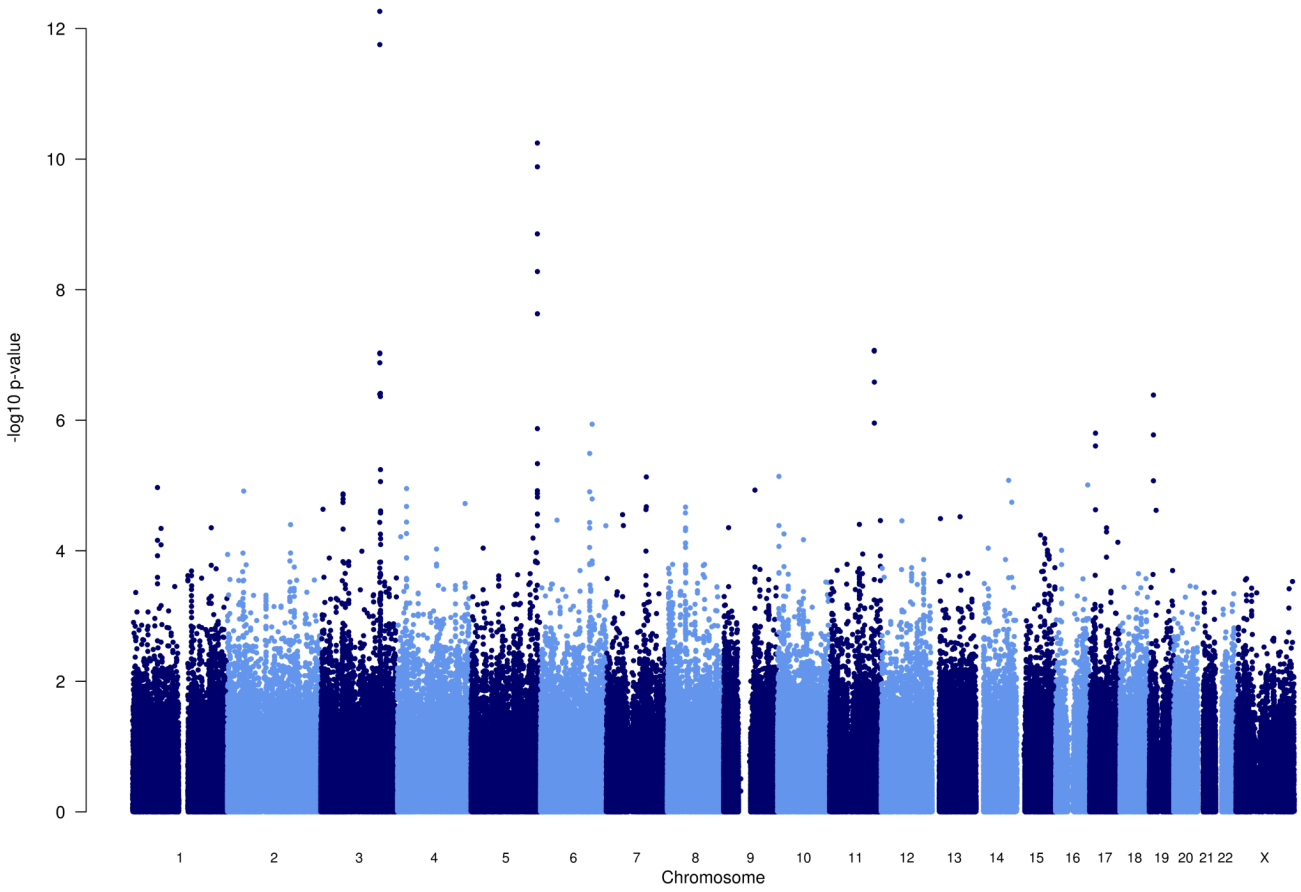

Figure 1.
Manhattan plot of GWAS for IHPS. The genome-wide distribution of −log10 P values after correction by genomic control (λ=1.06) is shown across the chromosomes.

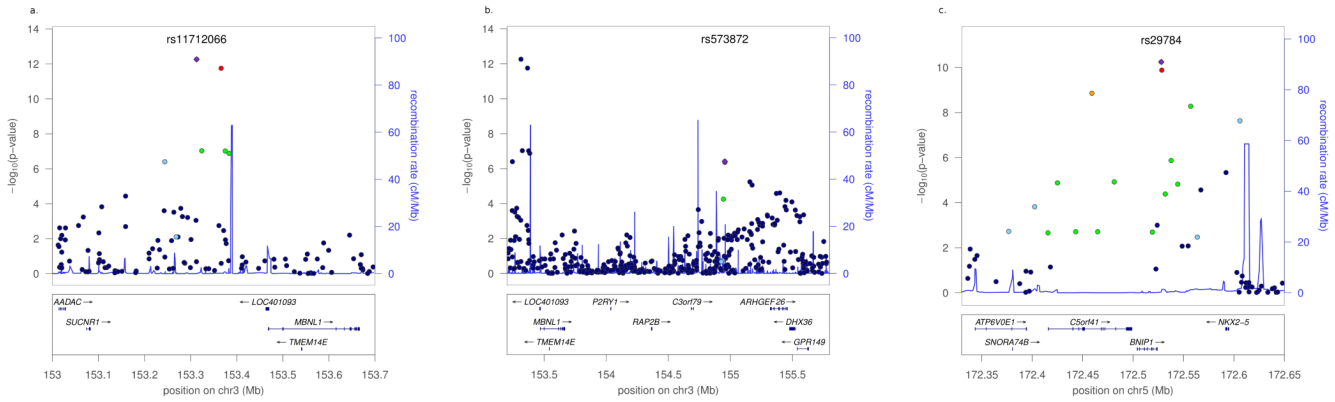

Figure 2.

Regional association plots for three confirmed novel IHPS loci. Association plots for the IHPS loci on a) chromosome 3q25.1, b) chromosome 3q25.2, and c) chromosome 5q35.2. SNPs are plotted by chromosomal position (x-axis) against GWAS association with IHPS (–log10 P value). The strongest signal is labeled in the plot, and other SNPs are color coded to reflect their LD with the top SNP (based on pairwise r^2 values from the discovery stage data. Red: $r^2>0.8$; orange: $0.6<r^2<0.8$; green: $0.4<r^2<0.6$; light blue: $0.2<r^2<0.4$; purple: $r^2<0.2$). Estimated recombination rates (from HapMap) are plotted to reflect the local LD structure. Genes are indicated in the lower panel of each plot. The figure was generated using LocusZoom [27].

Table 1

Discovery, replication and combined results of the loci associated with IHPS. One SNP per region was followed up in the replication stage

		Position	Alleles			Frequency		Number		Odds Ratio		
chr	**SNP**	**(bp)**	**Eff**	**Alt**	**Sample Set**	**Cases**	**Controls**	**Cases**	**Controls**	**(95% CI)**	**P value**	**Het P**
3	rs11712066	153,312,999	A	G	Discovery	0.8307	0.7477	1,001	2,398	1.66 (1.44–1.90)	5.5e-13	
					Replication	0.8319	0.7638	699	872	1.53 (1.28–1.83)	2.7e-06	
					Combined			**1,700**	**3,270**	**1.61 (1.44–1.79)**	**1.5e-17**	**0.50**
3	rs573872	154,954,853	G	T	Discovery	0.2885	0.2285	1,000	2,400	1.37 (1.21–1.55)	3.9e-07	
					Replication	0.2915	0.2165	693	866	1.49 (1.27–1.75)	1.5e-06	
					Combined			**1,693**	**3,266**	**1.41 (1.28–1.56)**	**4.3e-12**	**0.42**
5	rs29784	172,527,914	A	G	Discovery	0.5395	0.4497	1,001	2,397	1.43 (1.29–1.60)	5.7e-11	
					Replication	0.5384	0.4545	690	868	1.40 (1.21–1.61)	3.3e-06	
					Combined			**1,691**	**3,265**	**1.42 (1.30–1.55)**	**1.1e-15**	**0.80**
6	rs1208285	134,200,493	C	T	Discovery	0.4573	0.3915	995	2,392	1.31 (1.17–1.46)	1.2e-06	
					Replication	0.4206	0.3882	693	863	1.14 (0.99–1.32)	0.07	
					Combined			1,688	3,255	1.25 (1.14–1.36)	6.2e-07	0.14
11	rs11216185	116,288,184	G	T	Discovery	0.0884	0.0527	1,001	2,401	1.74 (1.42–2.14)	8.5e-08	
					Replication	0.0675	0.0538	689	873	1.27 (0.95–1.71)	0.11	
					Combined			1,690	3,274	1.57 (1.33–1.86)	1.4e-07	0.09
19	rs2228671	11,071,912	T	C	Discovery	0.1396	0.0963	999	2,398	1.52 (1.29–1.79)	4.1e-07	
					Replication	0.1230	0.1208	699	865	1.02 (0.82–1.27)	0.85	
					Combined			1,698	3,263	1.32 (1.15–1.50)	3.7e-05	0.004

Eff, effect allele; Alt, alternative allele; Frequency, effect allele frequency; CI, confidence interval; Het P, P value for test of heterogeneity using the I^2 statistic.